



Spatial and seasonal patterns of water isotopes in northeastern German lakes

Bernhard Aichner¹, David Dubbert², Christine Kiel³, Katrin Kohnert³, Igor Ogashawara³,
Andreas Jechow^{2,3}, Sarah-Faye Harpenslager¹, Franz Hölker², Jens Christian Nejstgaard³,
Hans-Peter Grossart^{3,4}, Gabriel Singer^{2,5}, Sabine Wollrab³, and Stella Angela Berger³

¹Dept. 2 Community and Ecosystem Ecology, Leibniz Institute of Freshwater Ecology and Inland Fisheries,
Müggelseedamm 301, Berlin, Germany

²Dept. 1 Ecohydrology and Biogeochemistry, Leibniz Institute of Freshwater Ecology and Inland Fisheries,
Müggelseedamm 310, Berlin, Germany

³Dept. 3 Plankton and Microbial Ecology, Leibniz Institute of Freshwater Ecology and Inland Fisheries,
Zur alten Fischerhütte 2, 16775 Stechlin, Germany

⁴Institute for Biochemistry and Biology, Potsdam University, Maulbeerallee, 14469 Potsdam, Germany

⁵Department of Ecology, Innsbruck University, Technikerstrasse 25, 6020 Innsbruck, Austria

Correspondence: Bernhard Aichner (bernhard.aichner@gmx.de)

Received: 21 September 2021 – Discussion started: 7 October 2021

Revised: 4 March 2022 – Accepted: 9 March 2022 – Published: 19 April 2022

Abstract. Water stable isotopes ($\delta^{18}\text{O}$ and $\delta^2\text{H}$) were analyzed in samples collected in lakes, associated with riverine systems in northeastern Germany, throughout 2020. The dataset (Aichner et al., 2021; https://doi.org/10.1594/PANGAEA.935633) is derived from water samples collected at (a) lake shores (sampled in March and July 2020), (b) buoys which were temporarily installed in deep parts of the lake (sampled monthly from March to October 2020), (c) multiple spatially distributed spots in four selected lakes (in September 2020), and (d) the outflow of Müggelsee (sampled biweekly from March 2020 to January 2021). At shores, water was sampled with a pipette from 40–60 cm below the water surface and directly transferred into a measurement vial, while at buoys a Limnos water sampler was used to obtain samples from 1 m below the surface. Isotope analysis was conducted at IGB Berlin, using a Picarro L2130-i cavity ring-down spectrometer, with a measurement uncertainty of $< 0.15\text{‰}$ ($\delta^{18}\text{O}$) and $< 0.0\text{‰}$ ($\delta^2\text{H}$). The data give information about the vegetation period and the full seasonal isotope amplitude in the sampled lakes and about spatial isotope variability in different branches of the associated riverine systems.

1 Introduction

The varying physical properties of stable oxygen and hydrogen isotopes of the water molecule (^{16}O , ^{17}O , ^{18}O , ^1H , ^2H) result in isotope fractionation during evaporation and condensation processes. This causes spatial and temporal variability in the isotopic signature of water in both the liquid and the vapor phase (Craig, 1961; Dansgaard, 1964; Gat and Gorfantini, 1981). Water stable isotopes are therefore ideal tracers of hydrological processes, for example in lacustrine and riverine systems. Specifically in lakes, their general morphology (water volume, lake area, depth, and shape), the

mean residence time of the water, the balance between in- and outflows of multiple types (surface water, groundwater, precipitation), and their connectivity to other water bodies are important parameters controlling isotope ratios (Herzceg et al., 2003; Bocanegra et al., 2013; Wu et al., 2015; Kang et al., 2017; Mass-Dufresne et al., 2021).

The northeastern part of Germany is characterized by a complex system of rivers and lakes. The connectivity of those lakes is an important influence on how ecological and chemical water properties are propagated along the river–lake network. Water isotopes are ideal proxies to identify spatial pat-

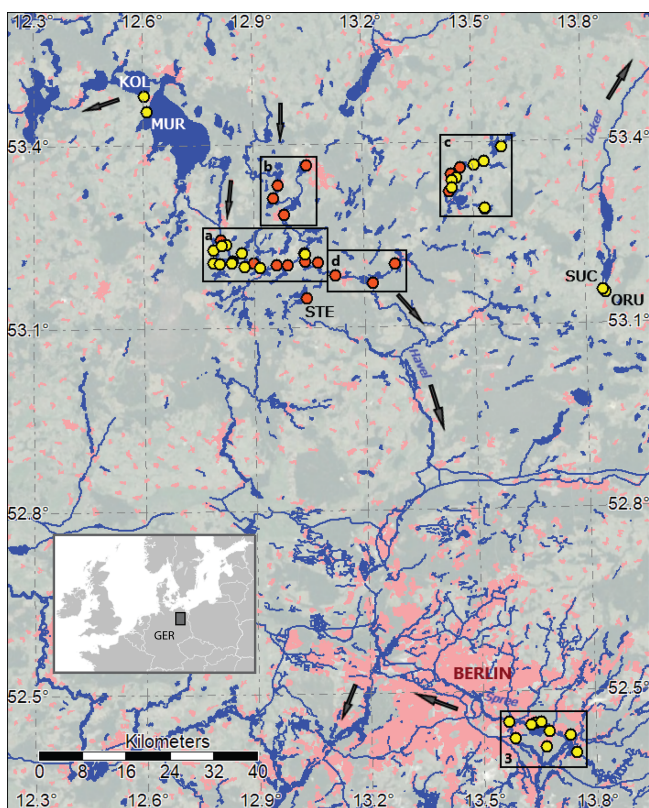


Figure 1. Sampling locations at lake shores (yellow) and buoys (red). Arrows indicate major flow directions of rivers. Black boxes refer to detailed maps in Figs. 2a–d and 3. The inset map indicates the location of the study area in Europe. Underlying map © Google Maps 2021.

terns within these coupled riverine and lacustrine systems and therefore a potential tool to assess lake-to-lake connectivity. So far, available isotope data from this region are limited to large rivers (Reckert et al., 2017), punctual snapshot data (Richter and Kowski, 1990), or small-scale patterns in local settings (Kuhleemann et al., 2020; Vyse et al., 2020; Kleine et al., 2021).

Here, we provide a comprehensive dataset of water isotopes in lakes along the river–lake system of the northeastern German lowland area (Aichner et al., 2021), which covers the major riverine systems and evaluates the seasonal variability on selected spots, i.e., in lakes which are part of different riverine branches of the investigated systems. The two major questions are (a) what the seasonal variability in water isotope values across the northeastern German lacustrine systems is and (b) whether there are spatial trends that can be unraveled by water isotope data.

For future regional studies, answers to these questions and the assessment of whether water stable isotopes can be used as an accurate proxy for lake-to-lake connectivity will be valuable in the context of the potential relationship between

hydrological, chemical, and biological properties of the studied systems.

2 Study site

Northeastern Germany, a section of the glacially formed North German Plain, is characterized by a complex system of rivers and 1000+ lakes (Fig. 1) with highly variable limnological features such as size, depth, shape, and biogeochemical properties (Ogashawara et al., 2020, 2021). Most of these inland waters are a part of the Elbe watershed, discharging into the North Sea, with the Spree–Dahme system and the Müritz–Havel system as major tributaries. Further to the northeast the Ucker system forms a major cluster of rivers discharging into the Baltic Sea. Smaller natural and artificial channels add to the complexity of this riverine and lacustrine network.

The study area is situated in the temperate climate zone with an annual precipitation and temperature of approximately 600 mm and 10 °C, respectively (Berlin; DWD, 2021). Isotope values of precipitation range from −84‰ (January) to −49‰ (July) for $\delta^2\text{H}$ and from −11.6‰ to −6.9‰ for $\delta^{18}\text{O}$ (OIPC, Online Isotopes in Precipitation Calculator; Bowen, 2022; Bowen et al., 2005; IAEA/WMO, 2022; Stump et al., 2014). Due to continental and altitude effects, i.e., isotopic depletion with progressive transport and rain-out of water vapor, δ values of precipitation isotopes decrease in the eastern part of Germany from the NW to the SE. This trend is mirrored in groundwater $\delta^2\text{H}$ values, which decrease in the study area from −60‰ in Lake Müritz to −63‰ in the Spree–Dahme rivers (Richter, 1987; Richter and Kowski, 1990).

Lakes sampled for this study are listed in Tables 1 and 2 and can be clustered into nine geographical groups: (I) Lake Müritz and Kölpinsee, which discharge via the Erpe towards the northwest to the Elbe (Fig. 1); (II) deep Müritz–Havel lakes, which discharge towards the southeast and east before the confluence with the upper Havel river in Priebertsee (Schwarzer See, Zethner See, Vilzsee, Zotzensee, Labussee, Rätzsee, Canower See, Kleiner Pälitzsee, Großer Pälitzsee) (Fig. 2a); (III) the mostly shallow upper Havel lakes, located north of the confluence with the Müritz–Havel waterways (Zierker See, Useriner See, Großer Labussee, Woblitzsee, Großer Priepertsee) (Fig. 2b); (IV) Havel lakes, east of the confluence (Ellbogensee, Ziernsee, Röblinsee, and Stolpsee) (Fig. 2d); (V) Großer Lychensee, which is connected via the river Woblitz with the Stolpsee; (VI) Feldberg lakes (Feldberger Haussee, Breiter Luzin, and Schmalter Luzin), which are connected with each other via surface flow but only via groundwater flow with the lakes of group V (Fig. 2c); (VII) lakes connected to the Ucker system, mostly via smaller creeks and artificial channels (Krewitzsee, Melensee, Wrechener See, Großer See, Große Lanke (southernmost sector of Oberuckersee), and Suckower Haussee)

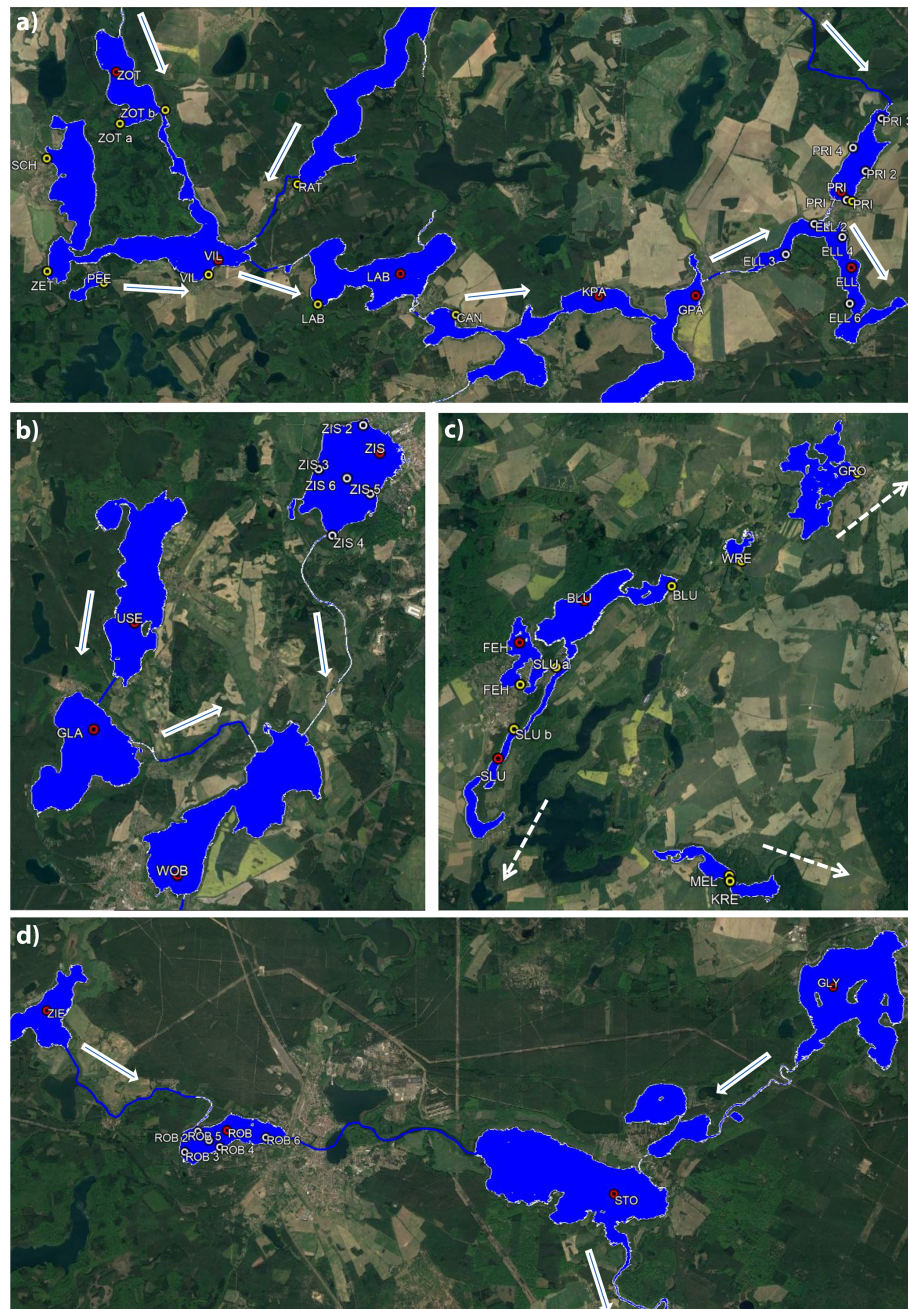


Figure 2. Sampling locations at (a) the Müritz–Havel, (b) the upper Havel, (c) Feldberg lakes, and (d) the Havel main branch. Shore samples taken in March and July 2020 are marked yellow. Time series samples from buoys in red. Spatial samples from lakes PRI, ELL, ZIS, and ROB in white. Arrows indicate streamflow direction. Underlying map © Google Earth 2021.

(Figs. 1 and 2c); (VIII) the Spree–Dahme system south-east of Berlin (Spree, Dämeritzsee, Große Krampe, Dahme, and Müggelsee) (Fig. 3); (IX) individual lakes Stechlin and Peetschsee, which are not connected to a major river but for which connectivity via groundwater flow and small artificial channels is partly still of relevance.

All of these sampled lakes show variable morphometric and ecological characteristics (Tables 1 and 2). The water

depths range from 3 m (Zierker See) to 70 m (Lake Stechlin) and the volumes from approximately 5.6×10^6 to $99.6 \times 10^6 \text{ m}^3$ (same lakes). By lake area, the investigated water bodies range from small ponds such as Peetschsee (19.1 ha) to the largest German lake, the Müritz (10910 ha). Most of the studied northeastern German lakes are mesotrophic or eutrophic according to the classification of LAWA (LAWA, 2014; Tables 1 and 2). Oligotrophic conditions only occur in

Table 1. Parameters of lakes with shore sampling spots (yellow dots in Fig. 1). Samples taken 40–60 cm below the water surface. Trophic class according to LAWA (2014) with the year of the most recent evaluation. Data from the respective German states were provided by local authorities (Landesamt für Umwelt Brandenburg, the Ministry of Agriculture and Environment Mecklenburg-Vorpommern); nd: no data.

Name	ID	Lat. (° N)	Long. (° E)	Sample date I (2020)	Sample date II (2020)	Area (ha)	Max. depth (m)	Volume (10 ⁶ m ³)	Residence time (yr)	Catchment (km ²)	Trophy index/class/year
Kölpinsee	KOL	53.480486	12.602401	10 Mar	19 Jul	2009	30.0	71.8	0.930	906	2.2/m2/2019
Müritz (Outer Müritz)	MUR	53.454812	12.609953	10 Mar	19 Jul	10 201	29.2	674.9	10.1	735	1.8/ml/2020
Schwarzer See	SCH	53.228292	12.788853	10 Mar	19 Jul	182	34.2	22.0	23.2	15	2.4/m2/2020
Zethner See	ZET	53.207225	12.789568	10 Mar	19 Jul	38.5	6.2	1.5	nd	20	3.1/e2/2017
Peetschsee	PEE	53.205068	12.807274	10 Mar	19 Jul	18.2	10.6	0.8	nd	1	3.1/e2/2016
Zotzensee a	ZOT	53.234774	12.811522	–	19 Jul	149.5	21.4	10.1	0.152	116	3.3/e2/2017
Zotzensee b	ZOT	53.237293	12.825709	10 Mar	19 Jul						
Vilzsee	VIL	53.206542	12.839634	10 Mar	19 Jul	200.2	21.7	15.9	0.229	147	3.2/e2/2017
Rätzsee	RAT	53.223299	12.867060	–	19 Jul	307.4	11.5	17.9	4.064	33	2.6/e1/2020
Labussee	LAB	53.200965	12.873554	–	19 Jul	258.3	26.4	18.3	0.223	210	2.9/e1/2014
Canower See	CAN	53.198937	12.916247	–	19 Jul	50.3	6.5	1.8	0.023	216	2.8/e1/2020
Großer Priepertsee	PRI	53.219635	13.039599	–	19 Jul	105.2	26.7	11.4	0.163	412	3.2/e2/2015
Schmaler Luzin a	SLU	53.325860	13.441056	08 Mar	16 Jul	146.2	33.5	21.2	3.359	30	1.4/o/2018
Schmaler Luzin b	SLU	53.341266	13.456269	08 Mar	16 Jul						
Feldberger Haussee	FEH	53.336906	13.441924	08 Mar	16 Jul	132.0	12.5	7.7	3.050	6	2.1/m2/2018
Breiter Luzin	BLU	53.361765	13.502401	08 Mar	16 Jul	337.3	58.3	76.9	16.254	23	1.9/ml/2018
Mellensee	MEL	53.290549	13.531495	08 Mar	16 Jul	73	18.3	5.4	5	93	2.1/m2/2019
Krewitzsee	KRE	53.289324	13.531882	08 Mar	16 Jul	57	18.8	4.1	1	117	2.3/m2/2019
Wrechener See	WRE	53.368161	13.531557	–	16 Jul	44.9	4.0	0.9	nd	12	2.6/e1/2019
Großer See	GRO	53.391470	13.580108	–	16 Jul	357	20	24	nd	69	3.2/e2/2017
Suckower Haussee	SUC	53.155456	13.847490	–	16 Jul	27	6.0	nd	nd	nd	2.7/e1/2018
Oberuckersee (Große Lanke)	ORU	53.149541	13.854400	08 Mar	16 Jul	540	28.5	57	4	329	1.8/ml/2017
River Spree b	SPREE	52.450164	13.567648	19 Mar	13 Jul						
River Dahme	DAHME	52.421870	13.585099	19 Mar	13 Jul						
Große Krampe	GRK	52.407561	13.666272	19 Mar	13 Jul	68	5.6	nd	nd	nd	nd
Müggelsee c (outflow)	MUG	52.444420	13.626031	19 Mar	13 Jul	746	7.7	36.6	0.14	6790	–/e1/2011
Müggelsee b	MUG	52.446808	13.638464	19 Mar	13 Jul						
Müggelsee a	MUG	52.448213	13.653171	19 Mar	13 Jul						
Müggelsee (inflow)	KLM	52.432557	13.676486	19 Mar	–						
Dämeritzsee	DAM	52.425817	13.730797	19 Mar	13 Jul	102.7	5.7	2.7	0.01	nd	–/e2/2011
River Spree a	SPREE	52.398384	13.747033	19 Mar	13 Jul						

the lake Schmaler Luzin. The water residence time in these lakes, i.e., the mean time that water spends in a particular lake, has been estimated by means of dividing the lake volume by the flow in or out of the lake (Wetzel, 2001). It ranges from a few weeks to few months in most river-connected lakes, while the Feldberg lakes and Lake Stechlin have longer residence times of ca. 3 to 16 years and > 60 years, respectively (Table 2).

3 Methods

3.1 Water sampling

Water samples were taken at the shore of 31 lacustrine and riverine spots from 40–60 cm water depth between 8–19 March and 13–19 July 2020 (Figs. 1–3; Table 1). At Müggelsee, samples were taken from a boat pier before the outflow on the northwestern side of the lake, in 2–4-week intervals between March 2020 and January 2021. Additionally, more samples were taken at two sites further east on the northern shore of the lake (Fig. 3) on 19 June

and 13 July 2020. Water samples were taken with a pipette and directly transferred in a gas chromatography (GC) vial, which was closed instantly after sampling and stored cold (6 °C) until further processing.

Between March and October 2020, water samples from a subset of 19 lakes (Table 2) were taken in 1–2-month intervals from a boat close to buoys, which were temporarily deployed as part of the project CONNECT at the deepest points of the lakes or (if a site coincided with a waterway) near the outflow of the lake (Ogashawara et al., 2020, 2021): 17–19 March, 25–28 May, 29 June–2 July, 3–6 August, 1–3 September, 5–8 October. On 29 and 30 September, four lakes (Zierker See, Großer Priepertsee, Ellbogensee, Röblinsee) were sampled at a higher spatial resolution by taking six or seven surface samples, distributed over the whole lake surface area at positions close to all shores, in addition to the sample at the deepest point and/or center of the lakes (Fig. 2).

A Limnos water sampler (Limnos, Komorów, Poland), capturing 2.5 L volume, was used to obtain water samples from 1 m depth. Samples were transferred into 10 L canis-

Table 2. Parameters of lakes equipped with buoys (red dots in Fig. 1). Samples taken from 1 m below the water surface. Trophy class according to LAWA (2014) with the year of the most recent evaluation. Data from the respective German states were provided by local authorities (Landesamt für Umwelt Brandenburg and the Ministry of Agriculture and Environment Mecklenburg-Vorpommern).

Name	ID	Lat. (° N)	Long. (° E)	Trophy index/ class/ year	Lake area (ha)	Volume (10 ⁶ m ³)	Catchment (km ²)	Residence time (yr)	Sample/ max. depth (m)	Sampling dates 2020
Zotensee	ZOT	53.244500	12.810111	3.3/e2/2017	149.5	10.1	116	0.152	20/21	18 Mar, 26 May, 30 Jun, 3 Aug, 1 Sep, 6 Oct
Vitzsee	VIL	53.209231	12.842569	3.2/e2/2017	200.2	15.9	147	0.229	14/21	18 Mar, 26 May, 30 Jun, 3 Aug, 1 Sep, 6 Oct
Labussee	LAB	53.206569	12.899061	2.9/e1/2014	258.3	18.3	210	0.223	17/26	17 Mar, 26 May, 30 Jun, 3 Aug, 1 Sep, 5 Oct
Kl. Pälitzsee (E basin)	KPA	53.202269	12.960511	2.9/e1/2014	132.9	7.0	224	0.075	22/26	19 Mar, 27 May, 2 Jul, 6 Aug, 3 Sep, 5 Oct
Gr. Pälitzsee (N basin)	GPA	53.202261	12.990519	2.6/e1/2014	82.4	6.5	242	0.077	13/15	19 Mar, 27 May, 2 Jul, 6 Aug, 3 Sep, 5 Oct
Stechlinsee	STE	53.147460	13.031148	2.2/m2/2019	412	99.6	26	65.0	69/70	17 Mar, 25 May, 1 Jul, 4 Aug, 10 Sep, 6 Oct
Zierker See	ZIS	53.365950	13.045639	3.7/p1/2018	351.0	5.7	23	1.128	2/3	17 Mar, 27 May, 29 Jun, 5 Aug, 3 Sep, 6 Oct
Usseriner See	USE	53.332739	12.967211	2.8/e1/2018	376.4	17.4	161	0.725	8/10	17 Mar, 28 May, 29 Jun, 3 Aug, 1 Sep, 6 Oct
Großer Labussee	GLA	53.312300	12.954881	2.8/e1/2018	335.6	13.8	176	0.559	8/12	17 Mar, 27 May, 29 Jun, 3 Aug, 3 Sep, 5 Oct
Woblitzsee	WOB	53.284919	12.982481	3.3/e2/2015	504.5	19.8	346	0.345	4/7	17 Mar, 27 May, 29 Jun, 3 Aug, 3 Sep, 5 Oct
Großer Priepertsee	PRI	53.221431	13.036339	3.2/e2/2015	105.2	11.4	412	0.163	16/27	18 Mar, 26 May, 1 Jul, 6 Aug, 3 Sep, 8 Oct
Ellbogensee	ELL	53.207319	13.038950	2.9/e2/2015	174.0	13.4	618	0.103	14/18	18 Mar, 26 May, 2 Jul, 6 Aug, 3 Sep, 8 Oct
Ziemsee	ZIE	53.205981	13.074319	2.8/e1/2013	112.0	6.8	634	0.052	12/13	18 Mar, 26 May, 2 Jul, 6 Aug, 3 Sep, 8 Oct
Röblensee	ROB	53.185311	13.120869	3.0/e2/2017	87	3.3	729	7.0	7/8	19 Mar, 25 May, 1 Jul, 4 Aug, 31 Aug, 7 Oct
Stolpsee	STO	53.171819	13.221836	3.0/e2/2017	371	24.7	1126	3.0	11/13	19 Mar, 25 May, 29 Jun, 4 Aug, 31 Aug, 7 Oct
Großer Lychnensee	GLY	53.202550	13.283633	3.3/e2/2017	282	17.6	175	3.0	19/19	–, 25 May, 29 Jun, 4 Aug, 31 Aug, 7 Oct
Schmaler Luzin	SLU	53.318739	13.435600	1.4/e2/2018	146.2	21.2	30	3.359	32/34	19 Mar, 28 May, 30 Jun, 5 Aug, 1 Sep, 8 Oct
Feldberger Haussee	FEH	53.347531	13.440081	2.1/m2/2018	132.0	7.7	6	3.050	12/13	19 Mar, 28 May, 30 Jun, 5 Aug, 1 Sep, 8 Oct
Breiter Luzin	BLU	53.358181	13.465839	1.9/m2/2018	337.3	76.9	23	16.254	56/58	19 Mar, 28 May, 30 Jun, 5 Aug, 1 Sep, 8 Oct

ters, closed after sampling, and immediately transported to the lab. Canisters were carefully turned upside down 10 times to guarantee constant mixing of samples before samples were transferred into GC vials with a pipette for isotope analysis. Vials were stored in a cold room (6 °C) in the dark until isotope measurement.

3.2 Isotope analysis

Water samples were filtered with 0.2 µm cellulose acetate (Faust Lab Science GmbH, Fabrikstraße 17, 79771 Klettgau, Germany) prior to analysis of stable isotopes ($\delta^{18}\text{O}$ and $\delta^2\text{H}$ values) in the water isotope lab at IGB Berlin using a L2130-i cavity ring-down spectrometer (Picarro, Santa Clara, CA, USA). All measurements were post-processed with the Picarro ChemCorrect™ software, which compared the measured spectra of the lab standards with the spectra of the samples. If statistical differences (i.e., baseline offset, spectral interference of organic compounds) between the two were too high, a warning flag was assigned, and the sample was excluded.

Isotope values and standard deviations are based on three replicate measurements of each sample, with three additional discarded measurements prior to avoid memory effects. To improve precision, all injections with a water concentration below 17 000 and above 23 000 ppm and with a standard deviation higher than 400 ppm of the measured water concentration across an injection's averaging window were excluded.

For instrument calibration three laboratory standards for each group of 24 samples were used: L ($\delta^{18}\text{O}$ –17.86‰ and $\delta^2\text{H}$ –109.91‰), DEL ($\delta^{18}\text{O}$ –10.03‰ and $\delta^2\text{H}$ –72.81‰), H ($\delta^{18}\text{O}$ 2.95‰ and $\delta^2\text{H}$ 0.29‰). A fourth lab standard, M ($\delta^{18}\text{O}$ –7.68‰ and $\delta^2\text{H}$ –56.70‰), was used as quality and drift control after every six samples, i.e., serving as lab-internal control and not being used for calibration. Mean values calculated from all measured M lab standards were –7.68‰ for $\delta^{18}\text{O}$ with a SD of 0.10‰ and –55.93‰ for $\delta^2\text{H}$ with a SD of 0.31‰. All lab standards were referenced against primary measurement standards: VSMOW2 (Vienna Standard Mean Ocean Water 2), GRESP (Greenland Summit Precipitation), and SLAP2 (Standard Light Antarctic Precipitation 2) from the IAEA (International Atomic Energy Agency, Vienna International Centre, 1400 Vienna, Austria).

Based on error propagation from (a) the uncertainty in reference lab standards, (b) root mean square errors in the calibrations, and (c) average standard deviation of replicate measurements of standards and samples, the overall measurement uncertainty in water isotope analysis was quantified to < 0.15‰ ($\delta^{18}\text{O}$) and < 0.40‰ ($\delta^2\text{H}$).



Figure 3. Sampling locations at the Spree–Dahme (SE Berlin). Time series samples from the Müggelsee outflow in red. Arrows indicate stream direction. Underlying map © Google Earth 2021.

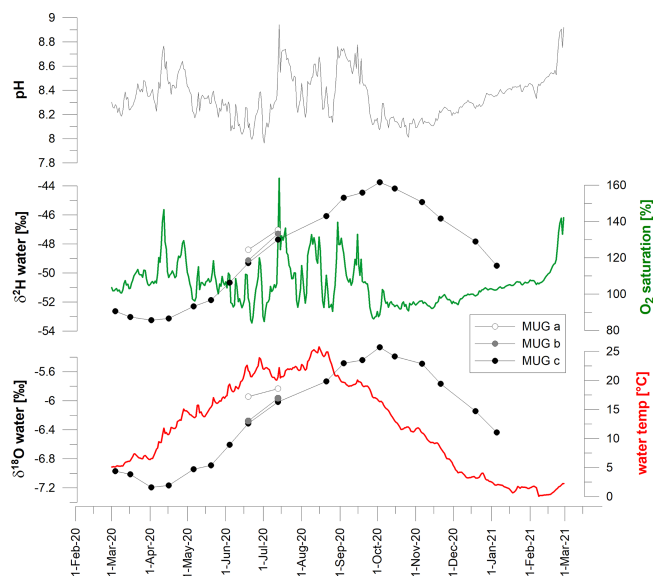


Figure 4. Time series of $\delta^2\text{H}$ and $\delta^{18}\text{O}$ values from the samples taken in 2–4-week intervals (March 2020–January 2021) at the outflow of Müggelsee (MUG c: Friedrichshagen harbor) and from additional samples taken on the northern shore (MUG a and b) on 19 June and 13 July. Water chemical and physical data are daily averages derived from the IGB long-term monitoring station (IGB, 2022).

4 Results and discussion

4.1 Time series

Isotopes exhibit a clear seasonal trend in the investigated lakes (Figs. 4 and 5). Minimum $\delta^2\text{H}$ and $\delta^{18}\text{O}$ values occur at the end of March/early April, while maximum values were measured at the end of September/early October. This is 6–8 weeks after the minimum and maximum water temperatures are reached and independent from the annual trends of water pH and O_2 saturation (Fig. 4). In the biweekly sampled Müggelsee, the isotope values vary from -53‰ to -44‰ ($\delta^2\text{H}$) and from -7.2‰ to -5.3‰ ($\delta^{18}\text{O}$), equivalent to seasonal isotope amplitudes of ca. 9‰ and 1.9‰ , respectively. The monthly sampled lakes showed variable seasonal amplitudes (i.e., offsets between October and March), ranging from $\delta^2\text{H}$ 2–13 ‰ (average: 4 ‰) and $\delta^{18}\text{O}$ 0.4–2.6 ‰ (average 0.9 ‰).

A seasonal isotopic signal has been observed in many riverine and lacustrine systems (e.g., Dutton et al., 2005; Ogrinc et al., 2012; Halder et al., 2015; Reckerth et al., 2017). Usually, the lake and river isotopes reflect the annual isotope trend of precipitation, but often with significant attenuation of the signal and a delay of 1–3 months (Rodgers et al., 2005; Jasechko et al., 2016; Reckerth et al., 2017; Bittar et al., 2016). This agrees with data from our study area, where precipitation isotopes reach their minimum and maximum in December/January and July/August, respectively, and exhibit

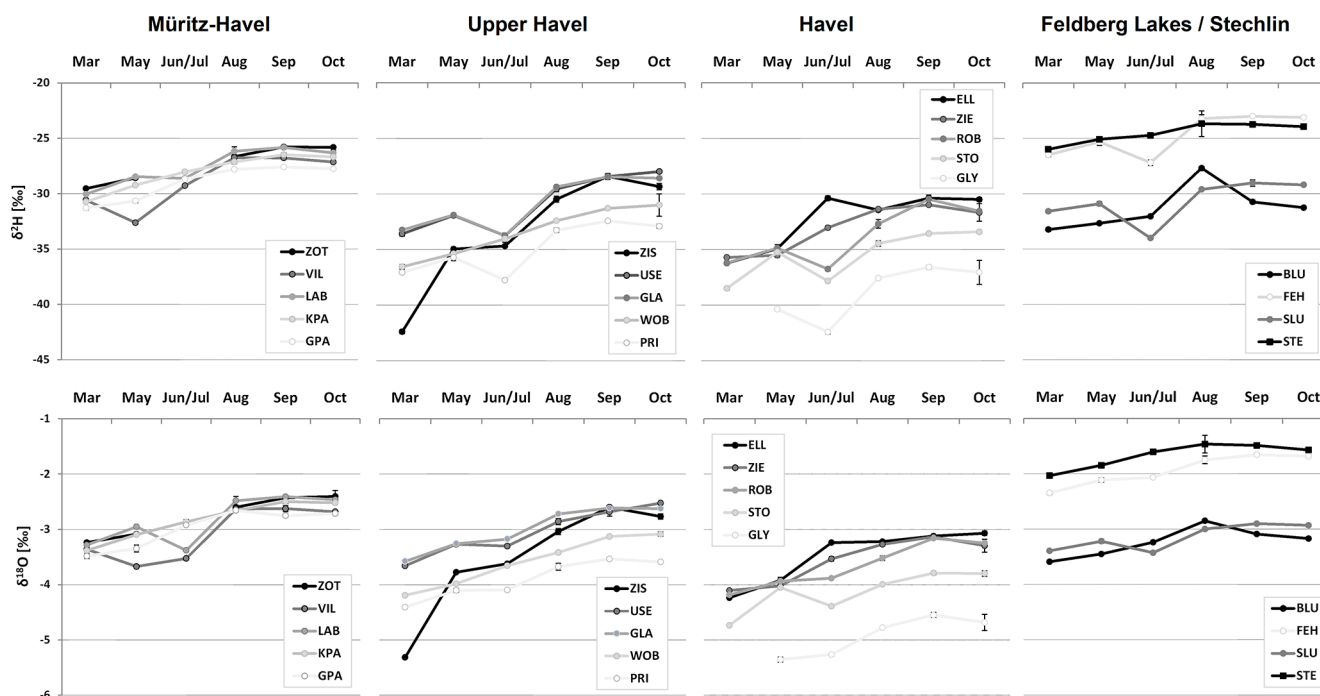


Figure 5. Time series of $\delta^2\text{H}$ and $\delta^{18}\text{O}$ values from March to October 2020. Water samples taken from 1 m depth at deepest water depths in lakes connected to the Müritz–Havel and upper Havel river systems and from the Feldberg lakes. Complementary water temperatures for each data point are available at PANGAEA.

a seasonal variability of ca. 35‰ ($\delta^2\text{H}$) and 4.7‰ ($\delta^{18}\text{O}$) (OIPC data for Berlin; Bowen et al., 2005; IAEA/WMO, 2022; Bowen, 2022). The reasons for the time delay between precipitation and river or lake water isotopes as well as the smaller seasonal amplitude of the latter can be attributed to multiple catchment characteristics and processes. Crucial influencing factors on how fast a precipitation isotope signal is transferred into fluvial systems are the discharge regime of rivers and the area and topography of their catchment (Sklash et al., 1976; Maloszewski et al., 1992; McGuire et al., 2005; Rodgers et al., 2005).

In our study area, the lowest seasonal (March–October) isotope variability was observed in Lake Stechlin, followed by the Feldberg lakes (Fig. 5), most likely due to their high water residence time and lack of connection to rivers (Table 2). In contrast, the highest amplitude is found in the shallow Zierker See, which also has the lowest volume of all studied lakes. Therefore it is most susceptible to summer evaporation with related isotopic enrichment of the lake water and also to inflow events, causing more negative values, as is visible in March (Fig. 5). Lake morphology can similarly explain the wide isotope amplitude of Müggelsee (Fig. 4), which is relatively large in area but also among the shallowest of the studied lakes. Data from most Havel lakes exhibited average seasonal isotope amplitudes (Figs. 5 and 7). The Spree–Dahme locations, Kölpinsee and Müritz, and the small Peetschsee showed relatively large deviations between

March and July (Fig. 7). All those lakes are either very shallow or have at least a large area-to-depth ratio.

These results show that the seasonal isotope amplitude is influenced by multiple characteristics of the studied lakes. Aside morphological parameters (lake area, depth, and volume), hydrological features (e.g., water residence time) are of importance.

4.2 Spatial patterns

In the four lakes with increased spatial coverage from September samples, little intra-lake variability in isotope values (0.5‰–1‰ for $\delta^2\text{H}$ and 0‰–0.2‰ for $\delta^{18}\text{O}$) was observed (Fig. 6). In contrast, along the transects, the multiple lakes showed an isotope variability of ca. 25‰ ($\delta^2\text{H}$) (Fig. 7) and of ca. 3‰ ($\delta^{18}\text{O}$).

In general, lakes showed decreasing δ values from the northwest (Müritz) towards the southeast (Spree–Dahme). This follows a similar spatial trend to isotopes in precipitation and groundwater (Richter, 1987; Richter and Kowski, 1990).

In addition, the lakes from the different geographical clusters can be distinguished according to their water isotope signatures: (I) the highest values were measured in the two lakes associated with the Müritz–Erpe system (I). The upper Havel is characterized by lower isotope values than the Müritz–Havel (II and III). The two lakes Schwarzer See and Zethner See are an exception, which show more negative values than

Table 3. Sampling locations for spatial campaigns in Zierker See (ZIS), Großer Priepertsee (PRI), Ellbogensee (ELL), and Röblinsee (ROB) (white dots in Fig. 2). Samples with ID no. 1 are identical to buoy samples as listed in Table 2 and taken from 1 m below the water surface.

Sampling date	Location	Latitude (° N)	Longitude (° E)	Secchi depth (m)	Water depth at sampling site (m)
29 Sep 2020	ZIS 1	53.365975°	13.045650°	0.45	2.7
29 Sep 2020	ZIS 2	53.371400°	13.040172°	0.35	1.3
29 Sep 2020	ZIS 3	53.362697°	13.025783°	0.4	1.3
29 Sep 2020	ZIS 4	53.349753°	13.030467°	0.45	0.7
29 Sep 2020	ZIS 5	53.357917°	13.042639°	0.4	0.8
29 Sep 2020	ZIS 6	53.360944°	13.035014°	0.5	1.95
29 Sep 2020	PRI 1	53.221492°	13.036342°	1	16
29 Sep 2020	PRI 2	53.225261°	13.044003°	1.1	> 10
29 Sep 2020	PRI 3	53.235164°	13.049375°	1	2.2
29 Sep 2020	PRI 4	53.229672°	13.040261°	1	5
29 Sep 2020	PRI 5	53.224444°	13.038806°	1.1	> 10
29 Sep 2020	PRI 6	53.224444°	13.038806°	1.1	7.2
29 Sep 2020	PRI 7	53.219894°	13.037950°	1.1	9.2
30 Sep 2020	ELL 1	53.207383°	13.038944°	1.8	14.3
30 Sep 2020	ELL 2	53.215461°	13.027700°	1.85	6.3
30 Sep 2020	ELL 3	53.209814°	13.018661°	1.9	10.5
30 Sep 2020	ELL 4	53.213000°	13.036328°	1.9	6.3
30 Sep 2020	ELL 5	53.209417°	13.033500°	1.75	8.2
30 Sep 2020	ELL 6	53.200639°	13.038172°	1.7	6
30 Sep 2020	ROB 1	53.185361°	13.120836°	1.2	5.3
30 Sep 2020	ROB 2	53.185428°	13.113164°	1.2	1.5
30 Sep 2020	ROB 3	53.182275°	13.109422°	1.2	2.8
30 Sep 2020	ROB 4	53.182753°	13.118769°	1.1	5.4
30 Sep 2020	ROB 5	53.183917°	13.115953°	1.2	5.8
30 Sep 2020	ROB 6	53.183853°	13.130997°	1.2	2.5

the other Müritz–Havel lakes (Fig. 7). Those form a chain of headwater lakes in the Müritz–Havel system, whose major inflow is north of Zotzensee (Fig. 2a). Schwarzer See is characterized by a comparably large mean residence time of lake water (Table 2) and is probably under increased influence of isotopically depleted groundwater. The influence of the different isotopic signatures of the two upper Havel branches is also visible at their confluence in Ellbogensee (Fig. 2a). Here, two samples, ELL 2 and ELL 3 (white squares in Fig. 6), taken before the upper Havel, show approximately 1‰ ^2H enrichment compared to the samples taken after the confluence. In general, the Havel lakes after the confluence (IV) carry a mixed isotope signature of the Müritz–Havel and upper Havel, with stronger influence of the first, depending on season (Figs. 5–7). Isotope depletion was observed towards the Stolpsee, probably due to the influence of the Lychen lakes (V), which discharge into the upper Havel at Stolpsee via the Woblitz river and which showed the most negative values of all sampled lakes in the upper Havel system (Figs. 5 and 7).

The Feldberg lakes (VI) are a group of lakes located approximately 35 km northeast of the upper Havel system and with insignificant surface connection to the adjacent lake systems. They are characterized by relatively high water residence time and slow surface flow from Feldberger Haussee

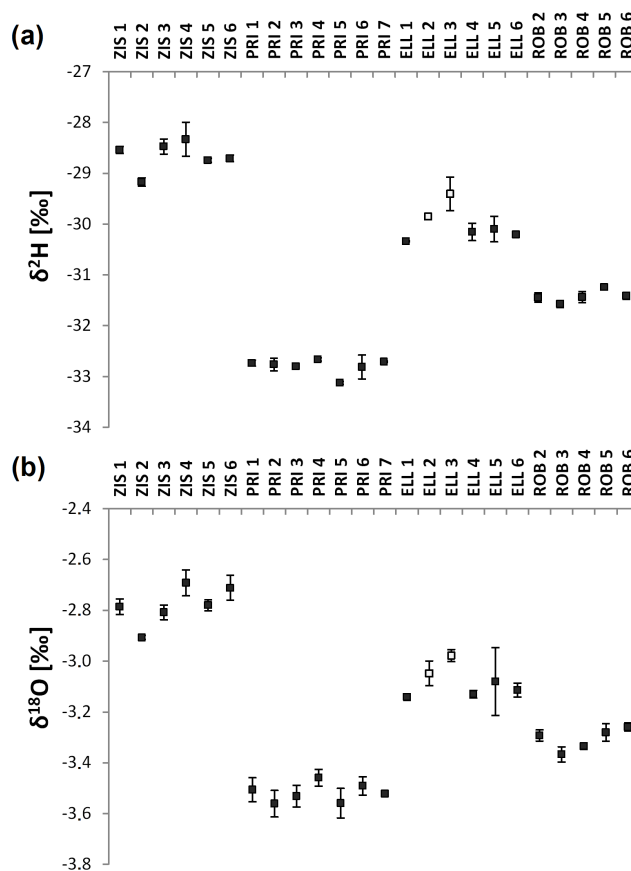


Figure 6. (a) $\delta^2\text{H}$ and (b) $\delta^{18}\text{O}$ values from samples taken at Zierker See (ZIS), Großer Priepertsee (PRI), Ellbogensee (ELL), and Röblinsee (ROB). For locations of samples refer to Table 3 and Fig. 2. White squares mark samples before the confluence with the upper Havel at Ellbogensee.

to Breiter Luzin and Schmalzer Luzin. $\delta^2\text{H}$ and $\delta^{18}\text{O}$ values are higher compared to the upper Havel and the main branch of the Havel (i.e., after the confluence at Großer Priepertsee and Ellbogensee), yet these are typical values of the Müritz–Havel. Among the three lakes, Feldberger Haussee shows the highest isotopic values, probably due to its lower water depth and volume (compared to Breiter and Schmalzer Luzin) and therefore increased susceptibility to evaporative isotope enrichment.

Variable isotope values are observable in the six sampled lakes associated with the Ucker lake–river system (VII). Complex subsurface and surface flow patterns, mostly via smaller creeks and channels, their wide geographical distribution, and variability in morphometric properties, can explain the isotopic heterogeneity in those lakes. A geographic trend, i.e., lower $\delta^2\text{H}$ and $\delta^{18}\text{O}$ values in the Oberuckersee (Große Lanke) compared to the more northern lakes (e.g., Mellensee, Krewitzsee), can be inferred from the data. The most negative isotope values in the study area were measured in samples from the lakes and rivers of the Spree–

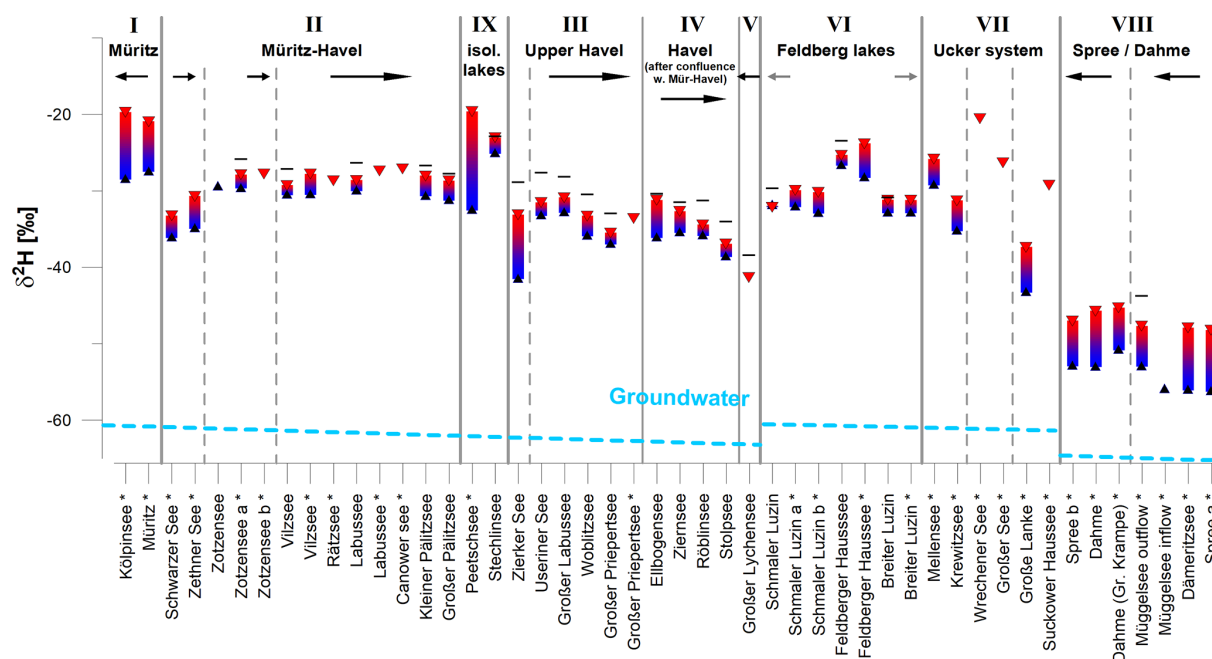


Figure 7. Seasonal variability in $\delta^2\text{H}$ values between spring (blue triangles) and summer (red triangles), framing the growing season of most aquatic and terrestrial plants. Additional data for autumn (black lines) indicate the full seasonal isotope amplitude. Samples taken at lake shores (*) and at buoys (1 m depth). Seasonal data represent samples taken in March, June/July, and October, respectively. Arrows mark the direction of surface (black) and subsurface flow (gray). Roman numbers indicate geographical clusters as described in Sect. 2. The vertical dashed gray line indicates sub-branches of these clusters (see Fig. 2). The dashed light-blue line indicates the approximate NW–SE trend in groundwater $\delta^2\text{H}$ values according to Richter (1987) and Richter and Kowski (1990).

Dahme system (VIII), located approximately 100 km south-east of the Müritz–Havel–Ucker systems.

The final group of lakes is characterized by low surface flow connectivity to riverine systems and other lakes (IX). Those lakes (Lake Stechlin and Peetschsee) show higher isotopic values than adjacent lakes and rivers, which can be attributed to evaporation effects. Those in turn are more pronounced in the smaller water bodies, which is visible from the large seasonal isotope amplitude in Peetschsee compared to small seasonal variability in the deep and large Lake Stechlin (Fig. 7).

5 Data availability

All data in this paper are available at PANGAEA: <https://doi.org/10.1594/PANGAEA.935633> (Aichner et al., 2021). This dataset is open for being extended in subsequent years.

6 Conclusions

Stable isotope $\delta^2\text{H}$ and $\delta^{18}\text{O}$ values of water samples collected in northeastern German lakes and rivers show clear spatial and seasonal trends. While isotope data exhibit a tendency from relatively high values in the northwest towards lower values in the southeast, evaporation and groundwater

inflow influence the isotope values on a local scale. In this context, morphometric parameters (water depth, area, volume, and overall shape) and related hydrological properties (water residence time, susceptibility to lake water evaporation and groundwater inflow) are crucial features, with effects on both absolute isotope values and their seasonal amplitude.

The comprehensive dataset of stable water isotopes and lake morphological characteristics described here can help to set biological and biogeochemical data in the context of hydrological processes in the northeastern German riverine and lacustrine systems. The ecological and chemical characteristics of these lake–river systems are driven by (a) connectivity between the lakes associated with river systems in addition to (b) local influencing factors, which in turn often depend on lake morphology. Water isotopes are able to reflect both those aspects, as shown by the different isotope patterns in the different branches of the Müritz–Havel–Ucker–Spree–Dahme system.

Author contributions. BA designed the isotope study and wrote the manuscript in close cooperation with the CONNECT project, coordinated by SAB and SW and performed by CK, AJ, KK, IO, JCN, HPG, FH, GS, SW, and SAB. DD analyzed water samples collected by BA, SFH, KK, CK, IO, AJ, SAB, SW, JCN, HPG, and

FH. All co-authors contributed to data evaluation and interpretation and editing of the manuscript.

Competing interests. The contact author has declared that neither they nor their co-authors have any competing interests.

Disclaimer. Publisher's note: Copernicus Publications remains neutral with regard to jurisdictional claims in published maps and institutional affiliations.

Acknowledgements. We thank Solvig Pinnow, Gregorio Lopez Moreira Mazacotte, Bianca Schmid-Paech, Fabian Göpel, Maren Lentz, and Gary Gottschall for help with sampling and sample preparation for isotope analysis. Funding was provided by the German Science Foundation (DFG) (project Ai 134/3-1). Part of this work was funded by the Leibniz Association within the Collaborative Excellence program for the project CONNECT – Connectivity and Synchronisation of Lake Ecosystems in Space and Time (K45/2017).

Financial support. This research has been supported by the Deutsche Forschungsgemeinschaft (grant no. Ai 134/3-1) and the Leibniz Association (grant no. K45/2017).

Review statement. This paper was edited by Attila Demény and reviewed by Gabriel Bowen and one anonymous referee.

References

- Aichner, B., Dubbert, D., Kiel, C., Kohnert, K., Ogashawara, I., Jechow, A., Harpenslager, S. F., Hölker, F., Singer, G., Grossart, H. P., Nejstgaard, J. C., Wollrab, S., and Berger, S. A.: Water isotope values from northeastern German lake systems 2020 et seq, PANGAEA [data set], <https://doi.org/10.1594/PANGAEA.935633>, 2021.
- Bittar, T. B., Berger, S. A., Birsa, L. M., Walters, T. L., Thompson, M. E., Spencer, R. G. M., Mann, E. L., Stubbins, A., Frischer, M. E., and Brandes, J. A.: Seasonal dynamics of dissolved, particulate and microbial components of a tidal saltmarsh-dominated estuary under contrasting levels of freshwater discharge, *Estuar. Coast. Shelf Sci.*, 182, 72–85, <https://doi.org/10.1016/j.ecss.2016.08.046>, 2016.
- Bocanegra, E., Quiroz Londoño, O. M., Martínez, D. E., and Romanelli, A.: Quantification of the water balance and hydrogeological processes of groundwater–lake interactions in the Pampa Plain, Argentina, *Environ. Earth Sci.*, 68, 2347–2357, <https://doi.org/10.1007/s12665-012-1916-4>, 2013.
- Bowen, G. J.: The Online Isotopes in Precipitation Calculator, version 3.1, <https://www.waterisotopes.org>, last access: 4 March 2022.
- Bowen, G. J., Wassenaar, L. I., and Hobson, K. A.: Global application of stable hydrogen and oxygen isotopes to wildlife forensics, *Oecologia*, 143, 337–348, <https://doi.org/10.1007/s00442-004-1813-y>, 2005.
- Craig, H.: Isotopic variations in meteoric waters, *Science*, 133, 1702–1703, <https://doi.org/10.1126/science.133.3465.1702>, 1961.
- Dansgaard, W.: Stable Isotopes in precipitation, *Tellus*, 16, 436–468, <https://doi.org/10.1111/j.2153-3490.1964.tb00181.x>, 1964.
- Dutton, A., Wilkinson, B. H., Welker, J. M., Bowen, G. J., and Lohmann, K. C.: Spatial distribution and seasonal variation in $^{18}\text{O}/^{16}\text{O}$ of modern precipitation and river water across the conterminous USA, *Hydrol. Process.*, 19, 4121–4146, <https://doi.org/10.1002/hyp.5876>, 2005.
- DWD: Klimadaten Deutschland, <https://www.dwd.de/DE/leistungen/klimadatendeutschland/klimadatendeutschland.html>, last access: 7 May 2021.
- Gat, J. R. and Gonfiantini, R. (Eds.): Stable Isotope Hydrology: Deuterium and Oxygen-18 in the Water Cycle, IAEA Technical Report Series No. 210, IAEA, Vienna, ISBN 92-0-145281-0, 1981.
- Halder, J., Terzer, S., Wassenaar, L. I., Araguás-Araguás, L. J., and Aggarwal, P. K.: The Global Network of Isotopes in Rivers (GNIR): integration of water isotopes in watershed observation and riverine research, *Hydrol. Earth Syst. Sci.*, 19, 3419–3431, <https://doi.org/10.5194/hess-19-3419-2015>, 2015.
- Herczeg, A. L., Leaney, F. W., Dighton, J. C., Lamontagne, S., Schiff, S. L., Telfer, A. L., and English, M. C.: A modern isotoperecord of changes in water and carbon budgets in a groundwater-fed lake: Blue Lake, South Australia, *Limnol. Oceanogr.*, 48, 2093–2105, <https://doi.org/10.4319/lo.2003.48.6.2093>, 2003.
- Jasechko, S., Kirchner, J. W., Welker, J. M., and McDonnell, J. J.: Substantial proportion of global streamflow less than three months old, *Nat. Geosci.*, 9, 126–129, <https://doi.org/10.1038/ngeo2636>, 2016.
- IAEA/WMO: Global Network of Isotopes in Precipitation, The GNIP Database, <https://nucleus.iaea.org/wiser>, last access: 4 March 2022.
- IGB: Müggelsee measuring station data, https://emon.igb-berlin.de/grosser_mueggelsee.html, last access: 4 March 2022.
- Kang, S., Yi, Y., Xu, Y., Xu, B., and Zhang, Y.: Water Isotope framework for lake water balance monitoring and modelling in the Nam Co Basin, Tibetan Plateau, *J. Hydrol. Reg. Studies*, 12, 289–302, <https://doi.org/10.1016/j.ejrh.2017.05.007>, 2017.
- Kleine, L., Tetzlaff, D., Smith, A., Goldammer, T., and Soulsby, C.: Using isotopes to understand landscape-scale connectivity in a groundwater-dominated, lowland catchment under drought conditions, *Hydrol. Process.*, 35, e14197, <https://doi.org/10.1002/hyp.14197>, 2021.
- Kuhlemann, L.-M., Tetzlaff, D., and Soulsby, C.: Urban water systems under climate stress: An isotopic perspective from Berlin, Germany, *Hydrol. Process.*, 34, 3758–3776, <https://doi.org/10.1002/hyp.13850>, 2020.
- LAWA: Trophieklassifikation von Seen, Richtlinie zur Ermittlung des Trophie-Index nach LAWA für natürliche Seen, Baggerseen, Talsperren und Speicherseen, Empfehlungen Oberirdische Gewässer, edited by: Riedmüller, U., Bund/Länder Arbeitsgemeinschaft Wasser, LAWA, Munich, Germany, ISBN 978-3-88961-345-5, 2014.

- Maloszewski, P., Rauert, W., Trimborn, P., Herrmann, A., and Rau, R.: Isotope hydrological study of mean transit times in an alpine basin (Wimbachtal, Germany), *J. Hydrol.*, 140, 343–360, [https://doi.org/10.1016/0022-1694\(92\)90247-S](https://doi.org/10.1016/0022-1694(92)90247-S), 1992.
- Masse-Dufresne, J., Barbecot, F., Baudron, P., and Gibson, J.: Quantifying floodwater impacts on a lake water budget via volume-dependent transient stable isotope mass balance, *Hydrol. Earth Syst. Sci.*, 25, 3731–3757, <https://doi.org/10.5194/hess-25-3731-2021>, 2021.
- McGuire, K. J., McDonnell, J. J., Weiler, M., Kendall, C., McGlynn, B. L., Welker, J. M., and Seibert, J.: The role of topography on catchment-scale water residence time, *Water Resour. Res.*, 41, W05002, <https://doi.org/10.1029/2004WR003657>, 2005.
- Ogashawara, I., Jechow, A., Kiel, C., Kohnert, K., Berger, S. A., and Wollrab, S.: Performance of the Landsat 8 provisional aquatic reflectance product for inland waters, *Remote Sens.*, 12, 2410, <https://doi.org/10.3390/rs12152410>, 2020.
- Ogashawara, I., Kiel, C., Jechow, A., Kohnert, K., Ruhtz, T., Grossart, H.-P., Hölker, F., Nejstgaard, J. C., Berger, S. A., and Wollrab, S.: The Use of Sentinel-2 for Chlorophyll-a Spatial Dynamics Assessment: A Comparative Study on Different Lakes in Northern Germany, *Remote Sens.*, 13, 1542, <https://doi.org/10.3390/rs13081542>, 2021.
- Ogrinc, N., Kanduc, T., Miljevic, N., Golobocanin, D., and Vaupotic, J.: Isotope Tracing of Hydrological Processes in River Basins: The Rivers Danube and Sava, in: *Monitoring Isotopes in Rivers: Creation of the Global Network of Isotopes in Rivers (GNIR)*, edited by: International Atomic Energy Agency, Vienna, Austria, ISBN 978-92-0-126810-5, 187–196, 2012.
- Reckerth, A., Stichler, W., Schmidt, A., and Stumpp, C.: Long-term data set analysis of stable isotopic composition in German rivers, *J. Hydrol.*, 552, 718–731, <https://doi.org/10.1016/j.jhydrol.2017.07.022>, 2017.
- Richter, W.: Deuterium and Oxygen-18 in Central European Groundwaters, *Isotopes Environ. Health Stud.*, 23, 385–390, <https://doi.org/10.1080/10256018708623855>, 1987.
- Richter, W. and Kowski, P.: Deuterium and Oxygen-18 in Surface Waters of GDR draining to the Baltic Sea, *Isotopes Environ. Health Stud.*, 26, 569–573, <https://doi.org/10.1080/10256019008622436>, 1990.
- Rodgers, P., Soulsby, C., Waldron, S., and Tetzlaff, D.: Using stable isotope tracers to assess hydrological flow paths, residence times and landscape influences in a nested mesoscale catchment, *Hydrol. Earth Syst. Sci.*, 9, 139–155, <https://doi.org/10.5194/hess-9-139-2005>, 2005.
- Sklash, M. G., Farvolden, R. N., and Fritz, P.: A conceptual model of watershed response to rainfall developed through the use of oxygen-18 as a natural tracer, *Can. J. Earth Sci.*, 13, 271–283, <https://doi.org/10.1139/e76-029>, 1976.
- Stumpp, C., Klaus, J., and Stichler, W.: Analysis of long-term stable isotopic composition in German precipitation, *J. Hydrol.*, 517, 351–361, <https://doi.org/10.1016/j.jhydrol.2014.05.034>, 2014.
- Vyse, S. A., Taie Semiromi, M., Lischeid, G., and Merz, C.: Characterizing hydrological processes within kettle holes using stable water isotopes in the Uckermark of northern Brandenburg, Germany, *Hydrol. Process.*, 34, 1868–1887, <https://doi.org/10.1002/hyp.13699>, 2020.
- Wetzel, R. G: *Limnology, Lake and River Ecosystems*, 3rd Edition, New York, Academic Press, ISBN 978-0-12-744760-5, 2001.
- Wu, H., Li, X., Li, J., Jiang, Z., Li, G., and Liu, L.: Evaporative enrichment of stable isotopes ($\delta^{18}\text{O}$ and δD) in lake water and the relation to lake-level change of Lake Qinghai, Northeast Tibetan Plateau of China, *J. Arid Land*, 7, 623–635, <https://doi.org/10.1007/s40333-015-0048-6>, 2015.